communications earth & environment

ARTICLE

https://doi.org/10.1038/s43247-022-00399-5 OPEN

Boundary conditions representation can determine simulated aerosol effects on convective cloud fields

Guy Dagan[1✉], Philip Stier[2], George Spill[2], Ross Herbert[2], Max Heikenfeld[2], Susan C. van den Heever[3] & Peter J. Marinescu[3,4]

Anthropogenic aerosols effect on clouds remains a persistent source of uncertainty in future climate predictions. The evolution of the environmental conditions controlling cloud properties is affected by the clouds themselves. Hence, aerosol-driven modifications of cloud properties can affect the evolution of the environmental thermodynamic conditions, which in turn could feed back to the cloud development. Here, by comparing many different cloud resolving simulations conducted with different models and under different environmental condition, we show that this feedback loop is strongly affected by the representation of the boundary conditions in the model. Specifically, we show that the representation of boundary conditions strongly impacts the magnitude of the simulated response of the environment to aerosol perturbations, both in shallow and deep convective clouds. Our results raise doubts about the significance of previous conclusions of aerosol-cloud feedbacks made based on simulations with idealised boundary conditions.

[1] Fredy and Nadine Herrmann Institute of Earth Sciences, Hebrew University, Jerusalem, Israel. [2] Atmospheric, Oceanic and Planetary Physics, Department of Physics, University of Oxford, Oxford, UK. [3] Department of Atmospheric Science, Colorado State University, Fort Collins, CO, USA. [4] Cooperative Institute for Research in the Atmosphere, Colorado State University, Fort Collins, CO, USA. ✉email: guy.dagan@mail.huji.ac.il

Aerosol, which serves as cloud condensation and ice nuclei, interacts with clouds and can impact their radiative, microphysical and dynamical properties[1]. These effects are known to be dependent on the cloud regime and environmental conditions[2–8]. However, since clouds interact with their environment, cloud adjustments due to aerosol perturbations can affect the evolution of the environmental thermodynamic conditions (such as water vapor and temperature vertical profiles) of both shallow[8,9] and deep-convective cloud fields[10,11]. The different environmental thermodynamic conditions could in turn affect the cloud properties[10,12] and hence substantially modify the magnitude of the total response from aerosol-cloud interactions (ACI).

In limited-area cloud-resolving model (CRM, including large eddy simulations—LES) simulations, some assumptions about the interaction between the domain and the larger-scale environment have to be made. Traditionally, boundary conditions (BCs) in CRM simulations are prescribed. The large-scale forcing (representing the BCs) may be kept constant in time[13,14], or change in time in a pre-defined gradual way[15,16]. In addition, it could be included by relaxing the domain mean temperature profile to a constant initial/baseline profile (under a weak temperature gradient assumption—WTG) and parametrizing the large-scale vertical motion[17–19], or be neglected entirely as in radiative-convective-equilibrium (RCE) simulations applying cyclic BCs[4]. We will refer to all these types of modeling set-ups here as "idealized simulations". Alternatively, temporally varying BCs based on realistic conditions from large-scale models, observations, or a combination of both, such as reanalysis data sets[5,11,20,21] are used. We will refer to these types of simulations here as "realistic simulations". We show below that this, apparently technical difference pertaining to model setup, can control the response of clouds to aerosol perturbations in simulations of both shallow and deep-convective cloud fields and attribute this to differences in the response of the atmospheric thermodynamic conditions.

A general tendency of humidification of the middle and upper troposphere due to aerosol perturbations of convective clouds has been shown before[5,11,22–25]. However, recently it was proposed, based on idealized simulations, that aerosol perturbations induce a very substantial increase of humidity at the middle and upper troposphere in the environment of tropical deep-convective clouds due to entrainment and enhanced mixing of condensed water into the surrounding air. This humidity increase then invigorates (i.e., increases the clouds' vertical velocities and precipitation) deep-convective clouds (ref. [10] —hereafter, referred to as AC21). The results of AC21 are based on equilibrium conditions in very long simulations (60 days) using idealized, time-independent BCs. This raises the question of whether more realistic atmospheric conditions would also demonstrate such a large humidity increase in response to aerosol perturbation.

Results and discussion

To address the above question, we compare in Fig. 1 the effect of aerosol on the water vapor mixing ratio (q_v) vertical profile from the idealized simulations of AC21 and 32 different realistic simulations conducted with 8 different models and microphysical schemes, under a wide range of environmental conditions (over ocean and land, in the tropics and extra-tropics), domain sizes (from 250 km to ~2000 km), grid resolutions (from 0.5 to 1.5 km) and simulation durations (from 12 hours to 8 days—see Methods for the full list of simulations). To account for variations in the applied aerosol perturbations between the different simulations, we normalize the difference between polluted and clean conditions to a factor of 10 increase in the cloud droplet number concentration or the aerosol number concentration (see Methods for details). Figure 1 clearly demonstrates that the increase in humidity shown in AC21 WTG simulations is at least an order of magnitude larger than the changes seen in the rest of the simulations. We also note that AC21 WTG simulations demonstrate a positive q_v change throughout the entire troposphere, and up to a doubling of the humidity at some of the levels under polluted conditions (Fig. 1b). This large increase raises questions about the possible source of this humidity in nature, as realistic changes are constrained by the atmospheric water budget[26]. In addition, such a large increase in humidity would have a very strong green-house effect. To evaluate this effect, we use a radiative transfer model (BUGSrad[27]). It demonstrates that the increase in humidity alone due to the aerosol perturbation simulated in AC21 WTG simulations leads to positive long-wave radiative forcing at the top of the atmosphere of 13.5 W/m^2, i.e., 3.5 times the effect of doubling the CO_2 concentration in the atmosphere. If occurring in nature, the associated substantial green-house effect should be observable.

We note that not all idealized representations of BCs will result in the same overestimation of the thermodynamic evolution. For example, in AC21 the two different set-ups used (WTG and RCE simulations) cause different humidity changes (see also Fig. S1, SI), and hence demonstrate different aerosol effects on cloud fields. Here, we focus on the WTG setup of AC21 as it was the basis of the proposed "humidity-entrainment" mechanism. The WTG setup, which generates a domain mean vertical velocity,

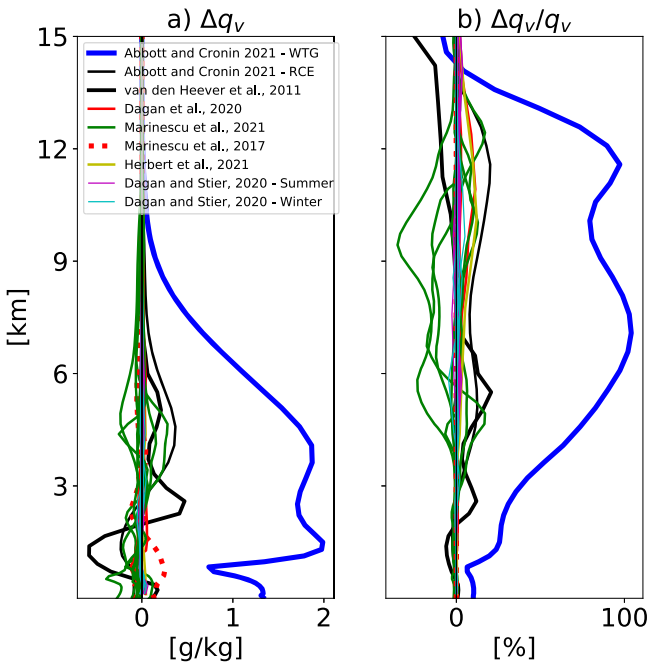

Fig. 1 Water vapor mixing ratio response to aerosol perturbation in deep-convective clouds simulations. Vertical profiles of the domain and time mean **a** change in water vapor mixing ratio—q_v, and **b** relative change in q_v due to an aerosol perturbation (normalized to an order-of-magnitude increase in aerosol concentration) from 34 different sets of simulations of deep-convective cloud fields representing a wide range of environmental conditions and produced by numerous different models. The blue curve presents results from idealized WTG simulations, black curves present results from idealized RCE simulations, whereas the rest of the curves are based on realistic simulations (the different green curves represent different models participated in Marinescu et al.[11], see Fig. 2 for a more detailed view of the realistic simulations). For details about the different simulations, please see the Methods section.

results in a substantially larger change in the humidity compared with the RCE simulations. Similarly, the RCE simulations of van den Heever et al.[4] demonstrate a much weaker humidity increase compared to AC21 WTG simulations (Figs. 1 and S1, SI). In equilibrium (as was simulated in AC21), the domain mean precipitation minus evaporation is set by the convergence of water vapor into the domain, which is determined by the representation of the BCs. In WTG simulations, this convergence is entirely determined by the local processes in the domain, without budgetary constraints[26]. However, under more realistic conditions, this term should, at least partially, be influenced by the larger-scale environment and be constrained by the availability of water vapor. For short simulations (sub-monthly) and on domain sizes smaller than 4000–5000 km (in which the atmosphere approaches RCE conditions[28,29]), a similar argument could also be presented for the atmospheric energy budget, i.e., realistic precipitation changes would be constrained by the ability of the atmosphere to radiatively cool and diverge the energy. The representation of BCs strongly impacts the energy divergence out of the domain, and hence also impacts the simulated aerosol effect on precipitation.

We now focus on the humidity changes in the realistic simulations and, as many of them are not discernible in the resolution presented in Fig. 1, Fig. 2 presents a zoomed-in version of Fig. 1. This demonstrates that in most of the realistic simulations, q_v increases in the middle and upper troposphere (above 3 km) under polluted conditions as has been shown previously[11,23]. This increase in humidity was shown before to be driven by suppression of warm rain formation in the lower troposphere and an increase in upwards water mass flux in clouds[11,23]. However, the increase is an order of magnitude smaller than the increase seen in AC21 WTG simulations. In addition, some of the simulations even predict a decrease in humidity at the middle and upper troposphere under polluted conditions.

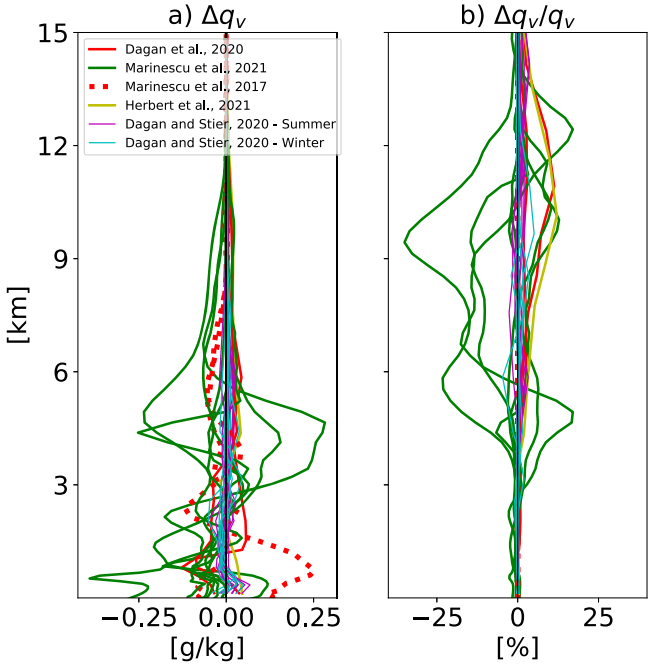

Fig. 2 Water vapor mixing ratio response to aerosol perturbation in realistic deep-convective clouds simulations. Vertical profiles of the domain and time mean **a** change in water vapor mixing ratio—q_v, and **b** relative change in q_v due to an aerosol perturbation (normalized to an order-of-magnitude increase in aerosol concentration). Same as Fig. 1 but focused only on the realistic simulations. The different green curves represent different models that participated in Marinescu et al.[11].

Since ACIs are time-dependent[12,30,31], we may expect the humidity increase to be affected by the length of the simulation. Figure 2 includes a diverse range of simulation durations (between 12 hours to 8 days), all demonstrating much smaller q_v changes than the idealized WTG simulations of AC21. Similarly, in realistic simulations, one may expect that the results would be domain size-dependent, as larger domain sizes reduce the role of the BC. The simulations presented above cover an order-of-magnitude range of domain sizes (250 km to 2000 km), and all of them demonstrate distinctly different behavior than the results of AC21 WTG simulations. In addition, the 2 RCE simulations presented in Fig. 1 were conducted using completely different domain sizes (10,000 km wide[4] compared with 128×128 km^2 in AC21), yet demonstrate similarly distinct responses compared to the WTG simulations. As AC21 pointed out, their results could be dependent on the initial/baseline conditions. We can evaluate this source of uncertainty using the simulations presented in Dagan and Stier (ref. [5]), where simulations were conducted with the same model, domain size, and simulation length but under a wide range of different baseline environmental conditions. The variation in the response seen between different baseline conditions in Dagan and Stier[5] (cyan and magenta curves in Fig. 2) is, again, drastically smaller than the difference between the WTG and the rest of the simulations.

Perhaps, the largest source of uncertainty of all may be due to model uncertainty[32], which can be evaluated using the multi-model ensemble simulations of the ACPC (Aerosol-Cloud-Precipitation-Climate international working group) deep convection intercomparison (green curves in Figs. 1 and 2 (ref. [11]), see Methods for details). These simulations include seven different models simulating a harmonized case study with near-identical model set-ups. Comparison of the different green curves in Fig. 2 demonstrates a large inter-model spread in the humidity response to aerosol perturbations, including negative and positive responses. However, all models show a distinctly weaker response compared to AC21 WTG simulations. The evaluation of this diverse collection of simulations suggests that the response of atmospheric humidity to aerosol perturbations, and the role of the so-called "humidity-entrainment" mechanism[10], is largely overestimated in the idealized WTG simulations of AC21. It also suggests that the representation of the BCs in deep convection simulations could strongly impact the effect of ACI on the thermodynamic conditions and hence also on the cloud properties.

To further demonstrate that the representation of the BCs in the different simulations is the key driver for the differences in the evolution of the thermodynamic conditions, we focus on the differences between the RCE and WTG simulations of AC21, as also shown in Fig. S1, SI. These simulations were conducted with the same model and microphysical scheme, for the same simulation duration and with a similar model setup, with only the representation of the BCs differing between the two simulations. The difference between the RCE and the WTG simulations of AC21 is as large as the differences between the WTG simulations and any of the other simulations presented in Fig. 1. Specifically, we note that the RCE simulations of AC21 and van den Heever et al. (2011) produce humidity responses to changing aerosol that is much more consistent than the humidity responses in WTG and RCE simulations of AC21 (conducted with the same model and similar setup beside the BCs representation). This suggests that the BCs representation is a key driver in determining the thermodynamic evolution, more so than the other modeling choices. The main difference between the WTG and the RCE set-ups is that the WTG setup generates a domain mean vertical velocity and can result in a large humidity convergence into the domain, while the RCE setup does not allow the exchange of

water between the domain and the outer domain. Thus, the WTG setup could result in a substantially larger change in the humidity compared with the RCE simulations.

Similar arguments were presented previously for the case of aerosol effects on shallow-convective cloud fields. Aerosol effects on shallow clouds have been shown to be time-dependent[9,12,20,33]. It has been suggested[9,24] that, given enough time for a cloud field to evolve, aerosol effects will be buffered, due to feedback between thermodynamic and microphysical processes. Specifically, the excess evaporation around the top of the cloudy layer under polluted conditions[22] drives deepening of the cloudy layer, hence, counteracting the warm rain suppression by aerosols[24] (as deeper clouds tend to precipitate more). This chain of processes may eventually bring the system to an equilibrium state in which the dependence of the domain-average properties, such as albedo and total rain, on the initial aerosol concentration is weak[9]. However, this equilibrium-state hypothesis was based on long idealized simulations in which the large-scale forcing (representing the BCs) was kept constant in time[9]. Through an analysis of equilibrium timescales from observations, it was shown that such equilibrium states are unrealistic in nature and that the BCs are expected to change fast enough to prevent cloud fields from reaching equilibrium[34]. This suggests that the representation of the BCs in shallow-convection simulations strongly impacts the effect of ACI on the thermodynamic conditions and that long-duration idealized shallow-convection simulations overestimate this effect.

Shallow-convection high-resolution models (CRM and LES) can also be configured to use realistic BCs, which change in time[5,20]. These types of simulations include a better representation of the natural evolution of the cloud fields in time, which is expected to affect the response of the clouds to aerosol perturbations[34]. Recently, a direct comparison of realistic and idealized simulations of shallow convection was conducted with a single model, the same domain mean baseline conditions, domain size, resolution, and simulation duration[35]. This demonstrated a much larger difference in the evolution of the thermodynamic conditions between polluted and clean conditions in idealized simulations compared to realistic simulations.

To further evaluate the effect of the BC setup on the thermodynamic evolution in shallow-convection, multi-model simulations under clean and polluted conditions, we compare 2 idealized and 43 realistic cases of shallow-convection simulated using a large range of initial conditions and simulation lengths (Fig. 3, c.f. Methods). The 2 idealized cases demonstrate a decrease in humidity near the surface and an increase in humidity in the upper part of the cloudy layer and inversion layer (the difference in the height of the level of the humidity increase in the two different cases is due to different cloudy layer depths, being much deeper in Spill et al.[35] compared to Dagan et al.[22]). Figure 3 demonstrates, similar to the case of deep convection, that the aerosol effect on the thermodynamic conditions and subsequent cloud evolution is overestimated in the simulations with idealized BCs compared with the realistic BCs.

Focusing on the realistic simulations, (Fig. 4) demonstrates that in all cases examined here, the aerosol perturbation drives a humidity decrease near the surface due to a reduction in rain evaporation[22], and an increase in humidity above the cloudy layer (3.5 km and above) due to increase in upward mass flux and evaporation, which is consistent with the general trends seen in the idealized LES and CRM simulations. However, the magnitudes of the humidity changes in the realistic simulations are much smaller than in the idealized simulations.

Focusing on the direct (single model) comparison of Spill et al. 2021 (Fig. S2, SI) suggests an order-of-magnitude larger humidity change in idealized simulations compared with realistic

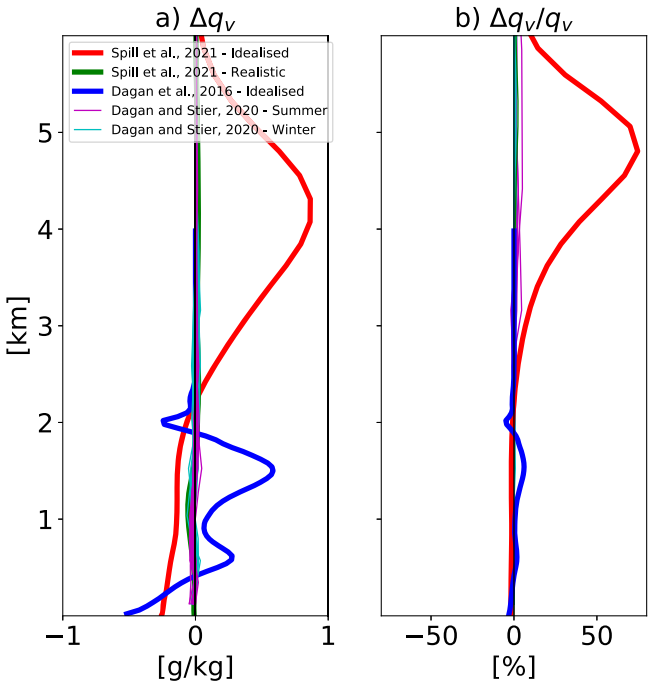

Fig. 3 Water vapor mixing ratio response to aerosol perturbation in shallow-convective clouds simulations. Vertical profiles of the domain and time mean **a** change in water vapor mixing ratio—q_v, and **b** relative change in q_v due to an aerosol perturbation (normalized to an order-of-magnitude increase in aerosol concentration) from 45 different sets of simulations of shallow-convective cloud fields representing a wide range of environmental conditions and produced by different models. The blue and red curves present results from simulations with idealized BCs, while the rest of the curves are based on realistic simulations (see Fig. 4 for a more detailed view). For details about the different simulations, please see the Methods section.

simulations, everything else being equal. The stronger similarity between the realistic simulations of Spill et al. 2021 and the other realistic simulations, compared to the humidity similarity with the idealized simulations, conducted with the same model and with a similar setup (besides the BCs representation) suggests, again, that the BCs representation is a key driver in determining the thermodynamic changes induced by aerosol perturbation, more than other modeling choices.

Conclusions

The humidity vertical profile evolution in limited-area CRM and LES simulations is shown here to be very sensitive to the representation of the BCs. Several processes exist which can affect the thermodynamic (humidity and temperature vertical profiles) evolution of a given region of the atmosphere, including large-scale advection, the diurnal cycle of solar radiation, surface fluxes, local radiative processes, and cloud processes. In many idealized simulations, the over-simplified representation of (usually time-invariant) advection into the domain, the lack of a diurnal cycle, and the use of periodic BCs result in an inflated role of the local cloud processes in setting the thermodynamic conditions. Hence, a change in cloud properties due to aerosol perturbations is manifested as a large change in the thermodynamic conditions. However, even between idealized set-ups, differences in the assumptions made (such as between WTG and RCE set-ups—Figs. 1 and S1, SI) can, to a large extent, determine the magnitude of the environmental thermodynamic evolution. The thermodynamic conditions are a key player in the clouds field evolution,

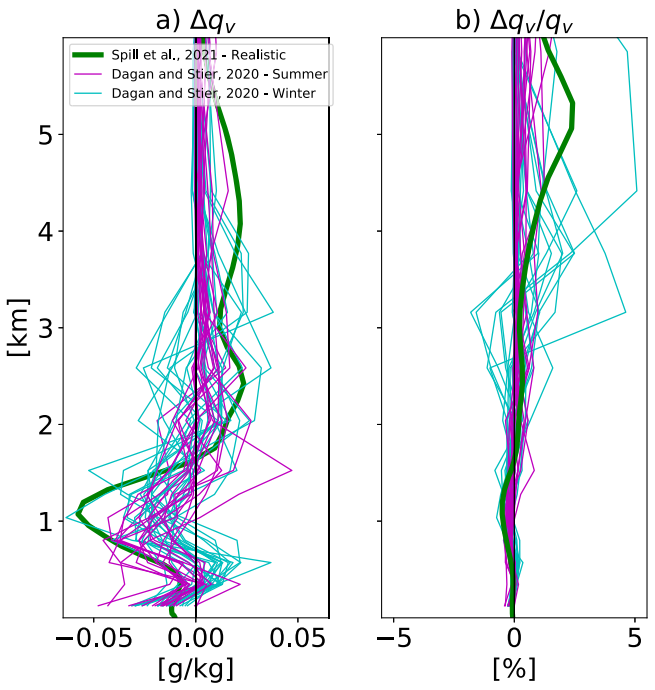

Fig. 4 Water vapor mixing ratio response to aerosol perturbation in realistic shallow-convective clouds simulations. Vertical profiles of the domain and time mean **a** change in water vapor mixing ratio—q_v, and **b** relative change in q_v due to an aerosol perturbation (normalized to an order-of-magnitude increase in aerosol concentration). Same as Fig. 3 but focused only on the realistic simulations.

hence, differences in the thermodynamic evolution due to aerosol perturbation are manifested as a large difference in the ACI response and clouds properties[10].

Our results show that some types of idealized BC representations overestimate the role of aerosol in the evolution of the environmental conditions, specifically the environmental humidity, in both shallow and deep-convective cloud fields when compared to more realistic BC simulations. Hence, the role of the recently proposed "humidity-entrainment" mechanism in deep-convective clouds (AC21) appears to be substantially overestimated (by an order of magnitude), due to the reliance on long WTG simulations. Similarly, the role of aerosols in deepening the boundary-layer, which was shown to buffer some of the aerosol effects on shallow clouds[9,24], also appears to be overestimated in idealized simulations[34,35]. In this paper, we have focused on the effect of aerosol on the humidity profile as it was recently highlighted[10], however, similar arguments could be presented for the case of the temperature evolution, and hence more broadly for the thermodynamic environment.

The results presented here emphasize the caution one should adopt in representing the BCs of cloud-resolving simulations when trying to quantify the role of different mechanisms for real-world conditions. Idealized simulations can certainly still be a useful tool to study and understand the underlying physical mechanisms of ACI. However, once a physical understanding is established based on the use of idealized simulations, conclusions for real-world conditions (and the assumptions behind the idealized setup) must be examined under more realistic simulation set-ups. The rise of global cloud-resolving models implicitly addresses the interactions between the large-scale circulation (specifically the advection of water and energy) and local ACI and hence could be transformative for the analysis and understanding of ACI.

Methods

For all simulations, we calculate the difference in the domain and time mean vertical profile of the water vapor mixing ratio (q_v) between clean and polluted conditions:

$$\triangle q_v = q_{v\,\mathrm{polluted}} - q_{v\,\mathrm{clean}} \quad (1)$$

and the vertical profile of the relative q_v change:

$$\triangle q_v / q_{v\,\mathrm{clean}} \quad (2)$$

To account for variations in the applied aerosol perturbations, we normalized the difference between polluted and clean conditions to a factor of 10 increase in the cloud droplet number concentration (N_c) or the aerosol number concentration (N_a)—depending on which one was presented in the relevant paper. We acknowledge that normalizing $\triangle q_v$ by N_a might result in a slightly smaller difference between polluted and clean conditions (compared to normalizing the results by N_c), as not all aerosols may be activated. However, this difference cannot explain the large differences seen between simulations with different BC representations, which are the focus of this work, and hence are not expected to significantly affect our conclusions.

For the comparison of the q_v changes in simulations of deep-convective clouds, data from 35 different simulated cases presented in 7 different published papers were used. Below we briefly summarize the simulations in each paper:

- Abbott and Cronin, (AC21)[10]: from AC21 we present the difference in the vertical profile of q_v based on their simulations conducted under the "weak temperature gradient" (WTG) approximation and under the "radiative-convective equilibrium" (RCE) assumption. Under the WTG approximation, diagnosed large-scale vertical motion acts to relax domain-average temperature profiles toward a reference profile. The reference temperature profile was set constant for all the different simulations. Under the RCE approximation, the BCs are neglected. AC21's simulations were performed using the System for Atmospheric Modeling (SAM[36]). Each simulation differed by the N_c. For a better comparison with the available N_c levels from Dagan et al. 2020 (ref. [23]) and Dagan and Stier, 2020 (ref. [5]), the N_c levels used here for representing polluted and clean conditions are 400 and 50 cm^{-3}, respectively, (the difference in q_v was then normalized to a factor of 10 increase). The data were downloaded from ref. [37]:
- Dagan et al.[23]: This study presents simulations of tropical cloud systems over a large domain (22° × 11°) centered in the tropical Atlantic Ocean. Two different sets of simulations, at different dates, were simulated with different baseline environmental conditions. Each case covered 48 hours, and N_c was varied. Here we use $N_c = 20\ \mathrm{cm}^{-3}$ and $N_c = 200\ \mathrm{cm}^{-3}$ as clean and polluted conditions, respectively. The simulations were conducted using the ICOsahedral Nonhydrostatic (ICON) atmospheric model[38]. The data used in this study can be found at ref. [39]:
- Dagan and Stier[5]: This study performed an ensemble of daily ICON simulations over 2-month-long periods in different seasons (December 2013 and August 2016). The domain is located east of Barbados and covers 3° × 3°. For each day, two simulations were conducted with $N_c = 20\ \mathrm{cm}^{-3}$ and $N_c = 200\ \mathrm{cm}^{-3}$, representing clean and polluted conditions, respectively. The resulting data set (consisting of 62 different simulated days) covers a large range of baseline meteorological conditions; hence, enabling estimation of the dependency of the q_v response to the initial conditions. For comparing the q_v changes in deep-convective cloud dominated conditions, we only used days that were identified as "deep-convective" dominated days in Dagan and Stier, 2020 (12 days during the summer month and 8 days during the winter month). The data used in this study can be found at ref. [40]:
- Marinescu et al.[11]: These studies present results from the Aerosol, Clouds, Precipitation and Climate (ACPC, http://acpcinitiative.org) initiative deep convection case study, a model intercomparison focusing on the response of deep-convective clouds to N_a perturbation. Seven state-of-the-art CRMs participated in this study. All models simulated the same case of deep-convective clouds near Houston, Texas using a harmonized setup (BCs, resolution, duration etc.). Each model was run with low and high N_a profiles, which are used here as the clean and polluted cases, respectively. The difference in N_a between the two cases is roughly a factor of 7.5[11]. We normalized the difference between polluted and clean conditions to a factor of 10 increase in N_a. As in Marinescu et al. 2021, the results presented here are based on the 12-hour period (1100–2300 local time) when deep-convective clouds were present in the observations and the highest resolution nested domain (500 m horizontal resolution). Further details about the different models and the setup can be found in Marinescu et al. 2021. All simulation data are stored and can be accessed on the UK CEDA JAMIN big data server: https://www.ceda.ac.uk/services/jasmin/.
- Herbert et al.[25]: This study presents very large domain (26° × 18°) CRM ICON simulations over the Amazon region with a simulation duration of 8 days. The goal of this paper was to isolate the responses of tropical deep-convective clouds to enhanced N_c (ACI) and changes in radiative fluxes (aerosol-radiation interactions). In this case, for comparison with AC21, we only use the simulations with the enhanced N_c (no direct or semi-direct

aerosol radiative effects). In the clean simulation $N_c = 100\ cm^{-3}$ throughout the domain. Unlike the previously mentioned simulations, the polluted case in this study uses a spatially inhomogeneous N_c enhancement based on the distribution of aerosols in the Max Planck Institute Aerosol Climatology version 2–Simple Plume model (MACv2-SP[41]). At the center of the aerosol plume $N_c = 830\ cm^{-3}$. We normalized the difference in q_v to an order of magnitude difference by multiplying by 1000/830 (normalizing by the domain mean N_c of $438\ cm^{-3}$, rather than the value at the center of the plume, does not significantly affect our results and the main conclusion). The data from this manuscript can be found at (Data for publication: "Isolating large-scale smoke impacts on cloud and precipitation processes over the Amazon with convection permitting resolution" 2021: https://doi.org/10.5281/zenodo.4445780).

- van den Heever et al.[4]: This study presents 2D RCE simulations conducted with the Regional Atmospheric Modeling System (RAMS[42]). The domain width was set to 10,000 km with 1 km resolution. A baseline simulation was allowed to reach equilibrium (which took ~60 days) after which aerosol perturbations were introduced. Each perturbed simulation was then run for another 40 days. The time-mean q_v vertical profiles presented here are based on the average over these 40 days in the simulations with $N_a = 100\ cm^{-3}$ and $N_a = 800\ cm^{-3}$ representing clean and polluted conditions, respectively. We normalized the difference in q_v to an order of magnitude difference in N_a.
- Marinescu et al.[43]: This study presents RAMS[44] simulations of two leading-line, trailing-stratiform midlatitude mesoscale convective system cases occurring during the MC3E Field Campaign[43,45,46] at 20 May 2011 (03–15 UTC), and 23 May 2011 (20–08 UTC). The analyses presented here utilize the output from within the inner, higher resolution nested domain, which has a grid resolution of 1.2 km. The results here are based on the 12-hour period in which the convective systems were active. We note that the domain sizes for these events are large (~7 × 13°) with respect to the convective system as these are fast-moving systems. Unlike the case of more homogeneous scattered convection, the averaging spatial scale could change the results. For consistency with the analysis of the rest of the simulations, we calculated the domain mean q_v vertical profile change. However, this is not expected to significantly affect our main conclusions and cannot explain the large difference between these simulations and the idealized WTG simulations of AC21. The polluted simulation utilized an aerosol profile with exponentially decreasing N_a with height (with a scale height of 7 km) from a surface N_a of $2000\ cm^{-3}$. The clean simulation utilized a similar shape of N_a vertical profile but with reduced vertical integrate concentration by ~70%. Here again, we normalized the difference in q_v to an order of magnitude difference in N_a.

For the comparison of q_v changes in simulations of shallow-convective clouds, data from 45 different simulated cases, presented in three different papers were used. We briefly summarize the simulations in each paper below:

- Dagan and Stier[5]: For comparison of the q_v changes in simulations of shallow-convective clouds we used the days that were identified as "shallow" and "two-layers" (shallow-convection with cirrus clouds above) dominated days in Dagan and Stier[5]. These simulations accounted for 42 out of the 62 days (23 days during the winter month and 19 days during the summer month). Additional information about these simulations is provided above.
- Spill et al.[35]: This study presents a direct comparison of idealized and realistic simulations of the Rain in Cumulus over the Ocean (RICO[47]) case study. These simulations were conducted with the Met Office Unified Model (UM) on relatively large domains of 500 km × 500 km. Each simulation was conducted for 4 days, whereas the analysis included all but the first 12 hours. The realistic setup used a nested domain, with BCs supplied by an external global configuration of the UM, which was run from operational analysis initial conditions. The idealized setup, on the other hand, used periodic boundaries, and constant large-scale forcing[48]. For a direct comparison between the two set-ups, domain mean profiles of temperature, humidity, and winds from the realistic simulations were used to initialize the idealized simulations. No interactive radiation is included in the idealized simulations presented here. The baseline (clean) aerosol profile was based on measurements of aerosol during RICO. For the polluted conditions, the aerosol profile was perturbed by a factor of 10. Data from these simulations is available at (Data for submitted publication: "Contrasting responses of idealised and realistic simulations of shallow cumuli to aerosol perturbations" 2021: https://doi.org/10.5281/zenodo.4726772).
- Dagan et al.[22]: This study performed idealized LES simulations of the Barbados Oceanographic and Meteorological Experiment (BOMEX[13]) case study conducted with SAM. The large-scale forcing was kept constant in time, the domain size was set to $12.8 \times 12.8 \times 4.0\ km^3$, and the simulation duration to 16 hours. In the clean case $N_a = 50\ cm^{-3}$, whereas in the polluted case $N_a = 500\ cm^{-3}$.

Data and materials availability

The raw data for many of the simulations is available as follows: T.H. Abbott, T.W. Cronin: data for "Aerosol invigoration of atmospheric convection through increases in humidity" (version 2), Zenodo (2020). https://doi.org/10.5281/zenodo.4071888.10.5281/zenodo.4071888. Dagan, G.: data of the paper: atmospheric energy budget response to idealized aerosol perturbation in tropical cloud systems [Data set], Zenodo, https://doi.org/10.5281/zenodo.3611366, 2020. Dagan, G. and Stier, P.: data of the paper: ensemble daily simulations for elucidating cloud-aerosol interactions under a large spread of realistic environmental conditions, Zenodo, https://doi.org/10.5281/zenodo.3785603, 2020. The simulation data of ref. [11] are stored and can be accessed on the UK CEDA JAMIN big data server: https://www.ceda.ac.uk/services/jasmin/. The simulation data of ref. [25] could be found at: https://doi.org/10.5281/zenodo.4445780. The simulation data of ref. [35] could be found at: https://doi.org/10.5281/zenodo.4726772.

Code availability

Any codes used in the paper are available upon request from: guy.dagan@mail.huji.ac.il.

Received: 11 September 2021; Accepted: 2 March 2022;
Published online: 28 March 2022

References

1. Bellouin, N. et al. Bounding global aerosol radiative forcing of climate change. *Rev. Geophys.* **58**, e2019RG000660 (2020).
2. Gryspeerdt, E. & Stier, P. Regime-based analysis of aerosol-cloud interactions. *Geophys. Res. Lett.* https://doi.org/10.1029/2012GL053221 (2012).
3. Christensen, M. W., Chen, Y. C. & Stephens, G. L. Aerosol indirect effect dictated by liquid clouds. *J. Geophys. Res. Atmos.* https://doi.org/10.1002/2016JD025245 (2016).
4. van den Heever, S. C., Stephens, G. L. & Wood, N. B. Aerosol indirect effects on tropical convection characteristics under conditions of radiative-convective equilibrium. *J. Atmos. Sci.* **68**, 699–718 (2011).
5. Dagan, G. & Stier, P. Stier. Ensemble daily simulations for elucidating cloud–aerosol interactions under a large spread of realistic environmental conditions. *Atmos. Chem. Phys.* https://doi.org/10.5194/acp-20-6291-2020 (2020).
6. Khain, A. P. Notes on state-of-the-art investigations of aerosol effects on precipitation: a critical review. *Environ. Res. Lett.* **4**, 015004 (2009).
7. Tao, W.-K., Chen, J.-P., Li, Z., Wang, C. & Zhang, C. Impact of aerosols on convective clouds and precipitation. *Rev. Geophys.* **50**, RG2001 (2012).
8. Storer, R. L., Van Den Heever, S. C. & Stephens, G. L. Modeling aerosol impacts on convective storms in different environments. *J. Atmos. Sci.* **67**, 3904–3915 (2010).
9. Seifert, A., Heus, T., Pincus, R. & Stevens, B. Large-eddy simulation of the transient and near-equilibrium behavior of precipitating shallow convection. *J. Adv. Model. Earth Syst.* https://doi.org/10.1002/2015MS000489 (2015).
10. Abbott, T. H. & Cronin, T. W. Aerosol invigoration of atmospheric convection through increases in humidity. *Science* **371**, 83–85 (2021).
11. Marinescu, P. J. et al. Impacts of varying concentrations of cloud condensation nuclei on deep convective cloud updrafts–a multimodel assessment. *J. Atmos. Sci.* https://doi.org/10.1175/JAS-D-20-0200.1 (2021).
12. Dagan, G., Koren, I., Altaratz, O. & Heiblum, R. H. Time-dependent, non-monotonic response of warm convective cloud fields to changes in aerosol loading. *Atmos. Chem. Phys.* **17**, 7435–7444 (2017).
13. Siebesma, A. P. et al. A large eddy simulation intercomparison study of shallow cumulus convection. *J. Atmos. Sci.* **60**, 1201–1219 (2003).
14. VanZanten, M. C. et al. Controls on precipitation and cloudiness in simulations of trade-wind cumulus as observed during RICO. *J. Adv. Model. Earth Syst.* https://doi.org/10.1029/2011MS000056 (2011).
15. Goren, T., Kazil, J., Hoffmann, F., Yamaguchi, T. & Feingold, G. Anthropogenic air pollution delays marine stratocumulus breakup to open cells. *Geophys. Res. Lett.* **46**, 14135–14144 (2019).
16. McGibbon, J. & Bretherton, C. Skill of ship-following large-eddy simulations in reproducing MAGIC observations across the northeast Pacific stratocumulus to cumulus transition region. *J. Adv. Model. Earth Syst.* **9**, 810–831 (2017).
17. Raymond, D. J. & Zeng, X. Modelling tropical atmospheric convection in the context of the weak temperature gradient approximation. *Q. J. R. Meteorol. Soc.* **131**, 1301–1320 (2005).
18. Sobel, A. H. & Bretherton, C. S. Modeling tropical precipitation in a single column. *J. Clim.* **13**, 4378–4392 (2000).
19. Warren, R. A., Singh, M. S. & Jakob, C. Simulations of radiative-convective-dynamical equilibrium. *J. Adv. Model. Earth Syst.* **12**, e2019MS001734 (2020).
20. Spill, G., Stier, P., Field, P. R. & Dagan, G. Effects of aerosol in simulations of realistic shallow cumulus cloud fields in a large domain. *Atmos. Chem. Phys.* https://doi.org/10.5194/acp-19-13507-2019 (2019).

21. Klocke, D., Brueck, M., Hohenegger, C. & Stevens, B. Rediscovery of the doldrums in storm-resolving simulations over the tropical Atlantic. *Nat. Geosci.* **10**, 891 (2017).
22. Dagan, G., Koren, I., Altaratz, O. & Heiblum, R. H. Aerosol effect on the evolution of the thermodynamic properties of warm convective cloud fields. *Sci. Rep.* **6**, 38769 (2016).
23. Dagan, G. et al. Atmospheric energy budget response to idealised aerosol perturbation in tropical cloud systems. *Atmos. Chem. Phys.* **20**, 4523–4544 (2020).
24. Stevens, B. & Feingold, G. Untangling aerosol effects on clouds and precipitation in a buffered system. *Nature* **461**, 607–613 (2009).
25. Herbert, R. J., Stier, P. & Dagan, G. Isolating large-scale smoke impacts on cloud and precipitation processes over the Amazon with convection permitting resolution. *J. Geophys. Res. Atmos.* https://doi.org/10.1029/2021JD034615 (2021).
26. Dagan, G., Stier, P. & Watson-Parris, D. Analysis of the atmospheric water budget for elucidating the spatial scale of precipitation changes under climate change. *Geophys. Res. Lett.* https://doi.org/10.1029/2019GL084173 (2019).
27. Stephens, G. L., Gabriel, P. M. & Partain, P. T. Parameterization of atmospheric radiative transfer. Part I: validity of simple models. *J. Atmos. Sci,* **58**, 3391–3409 (2001).
28. Jakob, C., Singh, M. & Jungandreas, L. Radiative convective equilibrium and organized convection: an observational perspective. *J. Geophys. Res. Atmos.* **124**, 5418–5430 (2019).
29. Dagan, G. & Stier, P. Constraint on precipitation response to climate change by combination of atmospheric energy and water budgets. *npj Clim. Atmos. Sci.* **3**, 1–5 (2020).
30. Glassmeier, F. et al. Aerosol-cloud-climate cooling overestimated by ship-track data. *Science* **371**, 485–489 (2021).
31. van den Heever, S. C., Carrió, G. G., Cotton, W. R., DeMott, P. J. & Prenni, A. J. Impacts of nucleating aerosol on Florida storms. Part I: mesoscale simulations. *J. Atmos. Sci.* **63**, 1752–1775 (2006). (2006).
32. White, B. et al. Uncertainty from choice of microphysics scheme in convection-permitting models significantly exceeds aerosol effects. *Atmos. Chem. Phys.* https://doi.org/10.5194/acp-17-12145-2017 (2017).
33. Lee, S.-S., Feingold, G. & Chuang, P. Y. Effect of aerosol on cloud–environment interactions in trade cumulus. *J. Atmos. Sci.* **69**, 3607–3632 (2012).
34. Dagan, G., Koren, I., Altaratz, O. & Lehahn, Y. Shallow convective cloud field lifetime as a key factor for evaluating aerosol effects. *iScience* **10**, 192–202 (2018).
35. Spill, G., Stier, P., Field, P. R. & Dagan, G. Contrasting responses of idealised and realistic simulations of shallow cumuli to aerosol perturbations. *Geophys. Res. Lett.* https://doi.org/10.1029/2021GL094137 (2021).
36. Khairoutdinov, M. F. & Randall, D. A. Cloud resolving modeling of the ARM summer 1997 IOP: model formulation, results, uncertainties, and sensitivities. *J. Atmos. Sci.* **60**, 607–625 (2003).
37. Abbott, T. H. & Cronin, T. W. Data for "Aerosol invigoration of atmospheric convection through increases in humidity" (version 2), Zenodo, 2020: https://doi.org/10.5281/zenodo.4071888.10.5281/zenodo.4071888.
38. Zängl, G., Reinert, D., Rípodas, P. & Baldauf, M. The ICON (ICOsahedral Non-hydrostatic) modelling framework of DWD and MPI-M: description of the non-hydrostatic dynamical core. *Q. J. R. Meteorol. Soc.* **141**, 563–579 (2015).
39. Dagan, G. Data of the paper: atmospheric energy budget response to idealized aerosol perturbation in tropical cloud systems [Data set], 2020: Zenodo, https://doi.org/10.5281/zenodo.3611366.
40. Dagan, G. & Stier, P. data of the paper: ensemble daily simulations for elucidating cloud–aerosol interactions under a large spread of realistic environmental conditions, Zenodo, https://doi.org/10.5281/zenodo.3785603, 2020.
41. Stevens, B. et al. MACv2-SP: a parameterization of anthropogenic aerosol optical properties and an associated Twomey effect for use in CMIP6. *Geosci. Model. Dev.* **10**, 433–452 (2017).
42. Cotton, W. R. et al. RAMS 2001: current status and future directions. *Meteorol. Atmos. Phys.* **82**, 5–29 (2003).
43. Marinescu, P. J. et al. The microphysical roles of lower-tropospheric versus midtropospheric aerosol particles in mature-stage MCS precipitation. *J. Atmos. Sci.* **74.11**, 3657–3678 (2017).
44. Saleeby, S. M. & van den Heever, S. C. Developments in the CSU-RAMS aerosol model: emissions, nucleation, regeneration, deposition, and radiation. *J. Appl. Meteorol. Climatol.* **52**, 2601–2622 (2013).
45. Marinescu, P. J., van den Heever, S. C., Saleeby, S. M. & Kreidenweis, S. M. The microphysical contributions to and evolution of latent heating profiles in two MC3E MCSs. *J. Geophys. Res. Atmos.* **121**, 7913–7935 (2016).
46. Saleeby, S. M., van den Heever, S. C., Marinescu, P. J., Kreidenweis, S. M. & DeMott, P. J. Aerosol effects on the anvil characteristics of mesoscale convective systems. *J. Geophys. Res. Atmos.* **121**, 10 880–10 901 (2016).
47. Rauber, R. M. et al. Rain in shallow cumulus over the ocean - the RICO campaign. *Bull. Am. Meteorol. Soc.* **88**, 1912–1928 (2007).
48. vanZanten, M. C. et al. Controls on precipitation and cloudiness in simulations of trade-wind cumulus as observed during RICO. *J. Adv. Model. Earth Syst.* **3**, M06001 (2011).

Acknowledgements

We acknowledge the ACPC-modeling groups for their roles in making available the ACPC multi-model data set. This work used JASMIN, the UK's collaborative data analysis environment (http://jasmin.ac.uk). This research was supported by the European Research Council (ERC) project constRaining the EffeCts of Aerosols on Precipitation (RECAP) under the European Union's Horizon 2020 research and innovation program with the grant agreement no. 724602. G.D. was supported by the Israeli Science Foundation Grant (1419/21). S.V. also acknowledges support from NASA grant 80NSSC18K0149. We thank Jiwen Fan for providing constructive comments during the preparation of this paper.

Author contributions

G.D. carried out the analyses presented and prepared the paper, with contributions from P.S., G.S., R.H., M.H., S.V., and P.J.M.

Competing interests

The authors declare no competing interests.

Additional information

Supplementary information The online version contains supplementary material available at https://doi.org/10.1038/s43247-022-00399-5.

Correspondence and requests for materials should be addressed to Guy Dagan.

Peer review information *Communications Earth & Environment* thanks Chunsong Lu and Nishant Nidhi for their contribution to the peer review of this work. Primary Handling Editor: Heike Langenberg. Peer reviewer reports are available.

Reprints and permission information is available at http://www.nature.com/reprints

Publisher's note Springer Nature remains neutral with regard to jurisdictional claims in published maps and institutional affiliations.